Selective cation and anion guest binding in host selenazamacrocycles

Upali Patel,[a] Mohammed A. Abbas,[a,b] Colin D. McMillen,[a] and Julia L. Brumaghim[a,*]

[a]Department of Chemistry, Clemson University, Clemson, SC 29634-0973, USA
[b]Department of Chemistry, Thi Qar University, Nasiriyah, Thi Qar, Iraq

SUPPLEMENTARY INFORMATION

Page

Experimental methods

Materials. Synthesis and manipulation of compounds were performed under argon atmosphere using standard air-free techniques. Acetonitrile and diethyl ether were purified using standard procedures and freshly distilled under argon prior to use. $Fe(BF_4)_2 \cdot 6H_2O$ (Sigma) was used as received. Selenazamacrocycles **5**[1] and **6**[2] were synthesized as reported.

Instrumentation. ^{1}H, $^{13}C\{^{1}H\}$, $^{19}F\{^{1}H\}$ and $^{77}Se\{^{1}H\}$ NMR spectra were collected on Bruker-AVANCE 300 and 500 MHz NMR spectrometers. ^{1}H, and $^{13}C\{^{1}H\}$ NMR chemical shifts are reported relative to tetramethylsilane (δ 0) and referenced to solvent. $^{19}F\{^{1}H\}$ NMR chemical shifts are reported relative to $CFCl_3$ (δ 0) and externally referenced to $NaBF_4$ (δ -150.4). $^{77}Se\{^{1}H\}$ NMR chemical shifts are externally referenced to diphenyldiselenide (δ 461[3]) and reported relative to dimethyl selenide (δ 0).

Infrared spectra were obtained from KBr pellets with a Magna 550 IR spectrometer. UV-vis spectra were collected using a Shimadzu UV-3101 PC spectrophotometer in quartz cuvettes with a 1 cm path length. MALDI mass spectrometry was performed on a Bruker Microflex mass spectrometer (accurate to ± 2 *m*/*z*) with *trans*-2-[3-(4-*tert*-butylphenyl)-2-methyl-2-propenylidene]malononitrile as the matrix. All peak envelopes matched calculated isotopic distributions. Elemental analysis was performed by Atlantic Microlabs, Inc.

Synthesis of complex ***7***. $Fe(BF_4)_2 \cdot 6H_2O$ (60 mg, 0.17 mmol) was dissolved in acetonitrile (5 mL) and this solution was cannula transferred into a solution of macrocycle **5** (100 mg, 0.16 mmol) in acetonitrile (25 mL). The reaction mixture was stirred at room temperature for 1 h and changed from colorless to dark brown. The solvent volume was reduced to 5 mL, and diethyl ether was diffused into the reaction mixture. The resulting dark-brown crystals of **7** were filtered and dried *in vacuo*. Yield 80% (112 mg). ^{1}H NMR (CD_3CN): δ 8.98 (s, 2H; CH=N), 8.86 (s, 2H;

CH=N), 7.95-7.85 (m, 4H; Ar-H), 7.72 (dt, 2H, J_{HH} = 8, 2.5 Hz; Ar-H), 7.63 (dd, 2H, J_{HH} = 8, 1.5 Hz; Ar-H), 7.54 (dt, 2H, J_{HH} = 7.5, 1 Hz; Ar-H), 7.28 (dt, 2H, J_{HH} = 7.5, 1.5 Hz; Ar-H), 7.25 (d, 2H, J_{HH} = 7.5 Hz; Ar-H), 6.75 (d, 2H, J_{HH} = 8 Hz; Ar-H), 4.40-4.25 (m, 4H; CH_2), 4.17-4.05 (m, 4H; CH_2). $^{13}C\{^1H\}$NMR (CD_3CN): δ 60.0 (CH_2), 62.4 (CH_2), 120.6 (Ar-C), 121.7 (Ar-C), 130.8 (Ar-C), 132.1 (Ar-C), 132.3 (Ar-C), 132.8 (Ar-C), 133.2 (Ar-C), 133.4 (Ar-C), 135.8 (Ar-C), 136.9 (Ar-C), 175.8 (CH=N), 176.5 (CH=N). $^{77}Se\{^1H\}$ NMR (CD_3CN): δ 438. IR (KBr, cm^{-1}): 3418 (b), 2925 (vs), 2856 (s), 1624 (s), 1581 (s), 1469 (s), 1435 (s), 1296 (s), 1223 (m), 1047 (b), 760 (vs), 521 (s), 445 (s). MALDI MS (*m*/*z*): 682 $[M\text{-}H^+]^+$, 701 $[M+OH]^+$. UV-vis, λ_{max}: 272, 450 (sh), 523, 557 (sh). Anal.calc. for $C_{32}H_{28}Se_2N_4FeB_2F_8$: C, 44.90; H 3.30; N, 6.55. Found: C, 44.68; H 3.43; N, 6.66.

*Synthesis of complex **8***. $Fe(BF_4)_2{\cdot}6H_2O$ (60 mg, 0.17 mmol) was dissolved in acetonitrile (5 mL) and the solution was cannula transferred to a solution of macrocycle **6** (106 mg, 0.16 mmol) in acetonitrile (25 mL). The reaction mixture was stirred at room temperature for 1 h and changed color from colorless to light yellow. The solvent volume was reduced to 15 mL and diethyl ether was diffused into the solution. Light-yellow crystals of **8** were filtered and physically separated from yellow-brown powder (characterized as $[Fe(NCCH_3)(O)(OH)]^-$ with *m*/*z* = 131 using negative-mode MALDI mass spectroscopy). Yield: 72% (97 mg). ^1H NMR (d_6-DMSO): δ 7.54 (br s; 4H, Ar-H), 7.39 (br s; 4H, Ar-H), 7.29 (br s, 4H), 7.24 (br s, 4H), 4.10 (br s, 8H, Ar-CH_2), 3.65 br, NH), 2.98 (br s, 8H, N-CH_2). $^{13}C\{^1H\}$ NMR (d_6-DMSO): δ 138.0 (Ar-C-Se), 134.6 (Ar-C), 133.5 (Ar-C), 130.9 (Ar-C), 129.9 (Ar-C), 128.6 (Ar-C), 52.0 (Ar-CH_2), 45.6 (N-CH_2). $^{19}F\{^1H\}$ NMR (d_6-DMSO) -148.72 ($^{10}BF_4^-$) and -148.76 ($^{11}BF_4^-$). $^{77}Se\{^1H\}$ NMR (d_6-DMSO): δ 330. IR (KBr) cm^{-1}: 3420 (b), 3328 (s), 3196 (s), 3134 (s), 3056 (s), 2838 (vs), 1601 (b,m), 1467 (m), 1443 (m), 1414 (m), 1398 (s), 1382 (s), 1251 (m), 1205 (m), 1113 (b,s),

1082 (b,s), 1061 (b,s), 1000 (b,m), 883 (w), 789 (s), 757(s), 653 (w), 596 (w), 521 (m), 473 (m). UV-vis, λ_{max}: 255 nm. MALDI MS (*m*/*z*): 727 $[M\text{-}BF_4]^+$. Anal. Calc. for $C_{32}H_{38}Se_2N_4B_2F_8$: C, 47.44; H 4.73; N, 6.92. Found: C, 47.64; H 4.89; N, 6.92.

Orbital calculations. The HOMO orbital surface of reduced macrocycle **6**[2] was generated via the single point energy calculation on the experimental crystal structure, using Gaussian09[4] at the MP2 level with the cc-pVTZ basis set. Clemson University is acknowledged for generous allotment of computational time on the Palmetto cluster.

X-ray data collection and structural determination. Single crystals of **7** and **8** were grown by vapor diffusion of diethyl ether into acetonitrile, mounted on a low-scatter loop using paratone, and immediately cooled to 100 ± 2 K in a cold nitrogen gas stream. Intensity data were collected using Mo Kα (λ = 0.71073 Å) radiation and a Photon 100 detector on a D8 Venture diffractometer (Bruker). Instrument control and data processing including integration (SAINT) and absorption correction and scaling (SADABS) were performed using the Apex3 software suite.[5] The space group for **7** and **8** was found to be $P2_1/n$ in both cases, based on the systematic absences. Structures were solved by direct methods and subsequent Fourier difference techniques, and refined anisotropically by full-matrix least-squares on F^2 using SHELXTL.[6] Details of the data collection and refinement are summarized in Table S1. The quantity minimized by the least squares program was $\sum w(F_o^2 - F_c^2)^2$ where $R_1 = [\sum|F_o| - |F_c|] / \sum|F_o|$; $wR_2 = \{[\sum w(F_o^2 - F_c^2]^2\}^{1/2}$. In the final cycle of least squares, independent anisotropic displacement parameters were refined for the non-hydrogen atoms, and hydrogen atoms were fixed in idealized positions using riding models based on the attached carbon atom. In the case of the protonated macrocycle of **8**, the presence of one hydrogen atom attached to N1 and two hydrogen atoms attached to N2 was first verified on the difference electron density map. These

hydrogen atoms were then freely refined using only a distance fixing restraint of 0.88 Å for the N-H distance. When crystals of **7** were grown using methanol instead of acetonitrile, solvent-free crystals of $[C_{32}H_{28}FeN_4Se_2][BF_4]_2$ were obtained, crystallizing in space group *C*2/*c* (Figure S2). These crystals had an improved air stability over the acetonitrile solvate, and the data were collected at room temperature and refined as above (Table S2). Selected bond lengths and angles for **7** and **8** (Table S3), selected bond lengths and angles for the solvent-free $[C_{32}H_{28}FeN_4Se_2][BF_4]_2$ (Table S4), and hydrogen bonds and close contact distances for **8** (Table S5) are summarized below. Packing diagrams for all complexes are provided in Figures S1, S3, and S4. A comparison of the unbound reduced marcrocycle and the tetrafluoroborate-coordinated reduced macrocycle is shown in Figure S5.

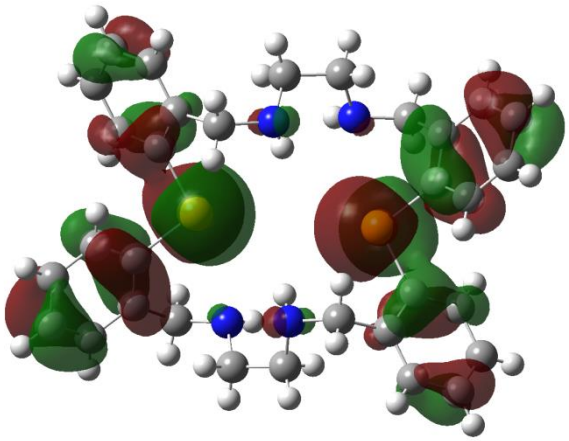

Figure S1. Calculated HOMO orbital surface for reduced macrocycle **6**.

Table S1. Crystallographic data for complexes **7** and **8**.

	7 $[C_{32}H_{28}FeN_4Se_2][BF_4]_2 \cdot 2(CH_3CN)$	**8** $[C_{32}H_{38}N_4Se_2][BF_4]_2$
Formula weight	938.08 g/mol	810.20 g/mol
Temperature	100(2) K	100(2) K
Wavelength	0.71073 Å	0.71073 Å
Crystal system, space group	Monoclinic, $P2_1/n$	Monoclinic, $P2_1/n$
a, Å	13.1966(5)	a = 14.941(2)
b, Å	17.7653(7)	b = 7.855(1)
c, Å	16.4051(6)	c = 15.117(2)
β, °	102.079(10)	107.334(4)
V, Å^3	3760.9(2)	1693.6(4)
Z, D_{cal} g/cm^3	4, 1.657	2, 1.589
μ, mm^{-1}	2.413	2.257
F(000)	1872.0	816
Crystal size, mm	0.037 × 0.235 × 0.244	0.036 × 0.038 × 0.161
Theta range for data collection, °	2.14-26.50	2.82 to 28.74
Index ranges	-15<=*h*<=16, -33<=*k*<=33, -19<=*l*<=20	-20<=*h*<=20, -10<=*k*<=10, -20<=*l*<=20
Reflections collected	47301	80008
Independent reflections	7794 [R(int) = 0.0335]	4386 [R(int) = 0.0498]
Max. and min. transmission	1.0000 and 0.6452	1.0000 and 0.9052
Refinement method	Full-matrix least-squares on F^2	Full-matrix least-squares on F^2
Data / restraints / parameters	7794 / 0 / 498	4386 / 3 / 229
Goodness-of-fit on F^2	1.200	1.081
Final *R* indices [I>2 σ(I)]	*R*1 = 0.0275, w*R*2 = 0.0767	*R*1 = 0.0266, w*R*2 = 0.0576
R indices (all data)	*R*1 = 0.0374, w*R*2 = 0.0930	*R*1 = 0.0319, w*R*2 = 0.0595
Weighting scheme	$w=1/[\sigma^2(F_o^2)+(0.0517P)^2+2.0365P]$ where $P=(F_o^2+2F_c^2)/3$	$w=1/[\sigma^2(F_o^2)+(0.0216P)^2+1.5023P]$ where $P=(F_o^2+2F_c^2)/3$
Largest diff. peak and hole	0.901 and -1.015 e·Å^{-3}	0.382 and -0.405 e·Å^{-3}

Table S2. Crystallographic data for solvent-free $[C_{32}H_{28}FeN_4Se_2][BF_4]_2$.

	$[C_{32}H_{28}FeN_4Se_2][BF_4]_2$
Formula weight	855.97
Temperature	298(2) K
Wavelength	0.71073 Å
Crystal system, space group	Monoclinic, *C*2/*c*
a, Å	a = 17.4674(17)
b, Å	b = 10.6360(11)
c, Å	c = 17.9626(19)
β, º	*β* = 106.425(3)
V, Å^3	3201.0(6)
Z, D_{cal} g/cm^3	4, 1.776
μ, mm^{-1}	2.824
F(000)	1696
Crystal size, mm	0.20 × 0.16 × 0.09
Theta range for data collection, °	2.39 to 25.15
Indexes range	-20<=*h*<=20, -12<=*k*<=12, -21<=*l*<=21
Reflections collected	13474
Independent reflections	2850 [R(int) = 0.0367]
Max. and min. transmission	1.0000 and 0.8668
Refinement method	Full-matrix least-squares on F^2
Data / restraints / parameters	2850 / 0 / 222
Goodness-of-fit on F^2	1.074
Final *R* indices [I>2 σ(I)] R_1 and wR_2	R_1 = 0.0496, wR_2 = 0.1144
R indices (all data) R_1 and wR_2	R_1 = 0.0636, wR_2 = 0.1286
Weighting scheme	$w=1/[\sigma^2(F_o^2)+(0.0527P)^2+16.2373P]$ where $P=(F_o^2+2F_c^2)/3$
Largest diff. peak and hole	1.034 and -0.452 e·Å^{-3}

Table S3. Selected bond lengths (Å) and angles (˚) for complexes **7** and **8**.

Complex **7**			
Se1-Fe1	2.3448(4)	N2-Fe1-N3	80.57(8)
Se2-Fe1	2.3657(4)	N4-Fe1-N1	79.46(8)
Fe1-N1	1.972(2)	N2-Fe1-N1	97.73(8)
Fe1-N2	1.962(2)	N3-Fe1-N1	91.06(9)
Fe1-N3	1.971(2)	N4-Fe1-Se1	91.24(6)
Fe1-N4	1.960(2)	N2-Fe1-Se1	90.32(6)
N4-C30	1.289(3)	N3-Fe1-Se1	170.81(6)
N2-C14	1.290(3)	N1-Fe1-Se1	88.92(6)
N1-C1	1.279(3)	N4-Fe1-Se2	88.65(6)
N3-C17	1.276(3)	N2-Fe1-Se2	94.07(6)
Se1-C8	1.922(3)	N3-Fe1-Se2	87.93(6)
Se1-C7	1.938(2)	N1-Fe1-Se2	167.83(6)
N4-Fe1-N2	176.76(9)	Se1-Fe1-Se2	94.002(14)
N4-Fe1-N3	97.79(8)	C8-Se1-C7	95.38(10)
		C24-Se2-C23	96.21(11)
Complex **8**			
N(2)-C(10)	1.506(2)	Se1-C1	1.928(16)
N(1)-C(7)	1.469(2)	Se1-C16#	1.932(16)
N(2)-C(9)	1.504(2)	C1-Se1-C16#	98.46(7)
N(2)-C(9)	1.504(2)	C10-N2-C9	114.98(12)
N(1)-C(8)	1.469(2)		

-x+1, -y+1, -z+1

Table S4. Selected bond lengths (Å) and angles (˚) for solvent-free $[C_{32}H_{28}FeN_4Se_2][BF_4]_2$.

$[C_{32}H_{28}FeN_4Se_2][BF_4]_2$			
Se1-Fe1	2.3533(9)	N2-Fe-N2#	176.3(3)
Fe1-N1 (x2)	1.973(5)	N1-Fe-N2	97.4(2)
Fe1-N2 (x2)	1.947(5)	N2-Fe-N1#	80.0(2)
N1-C1	1.279(8)	N1-Fe-N1#	91.1(3)
N2-C14	1.269(8)	N2-Fe-Se1#	92.72(14)
Se1-C8	1.924(5)	N2-Fe-Se1	89.79(15)
Se1-C7	1.930(5)	N1-Fe-Se1#	169.65(19)
		N1-Fe-Se1	88.45(19)
		Se1-Fe-Se1#	93.80(4)
		C8-Se1-C7	96.4(2)

-x, y, -z+1/2

Table S5. Hydrogen bond and close contact distances (Å) and angles (°) for **8**.

Bond	Donor-H	Acceptor-H	Donor…Acceptor	Angle
C8-H8A···F3	0.99	2.56	3.230(2)	125.0
C9-H9A···F1	0.99	2.62	3.253(2)	121.9
C9-H9A···F2	0.99	2.55	3.316(2)	134.1
C9-H9B···F4	0.99	2.57	3.126(2)	115.1
C10-H10B···F3	0.99	2.59	3.300(2)	128.3
C10-H10A···F1	0.99	2.34	3.1316(19)	136.1
N1-H1A···F1	0.863(15)	2.636(18)	3.3546(18)	141.5(18)
N1-H1A···F2	0.863(15)	2.384(18)	3.1329(19)	145.4(18)
N2-H2A···F1	0.860(15)	2.178(18)	2.8997(17)	141.3(19)
N2-H2A···N1	0.860(15)	2.34(2)	2.7881(19)	112.8(16)
N2-H2B···Se1	0.878(15)	3.091(19)	3.6198(14)	120.7(15)
N2-H2B···F3	0.878 (15)	1.951(16)	2.7589(19)	152.4(19)

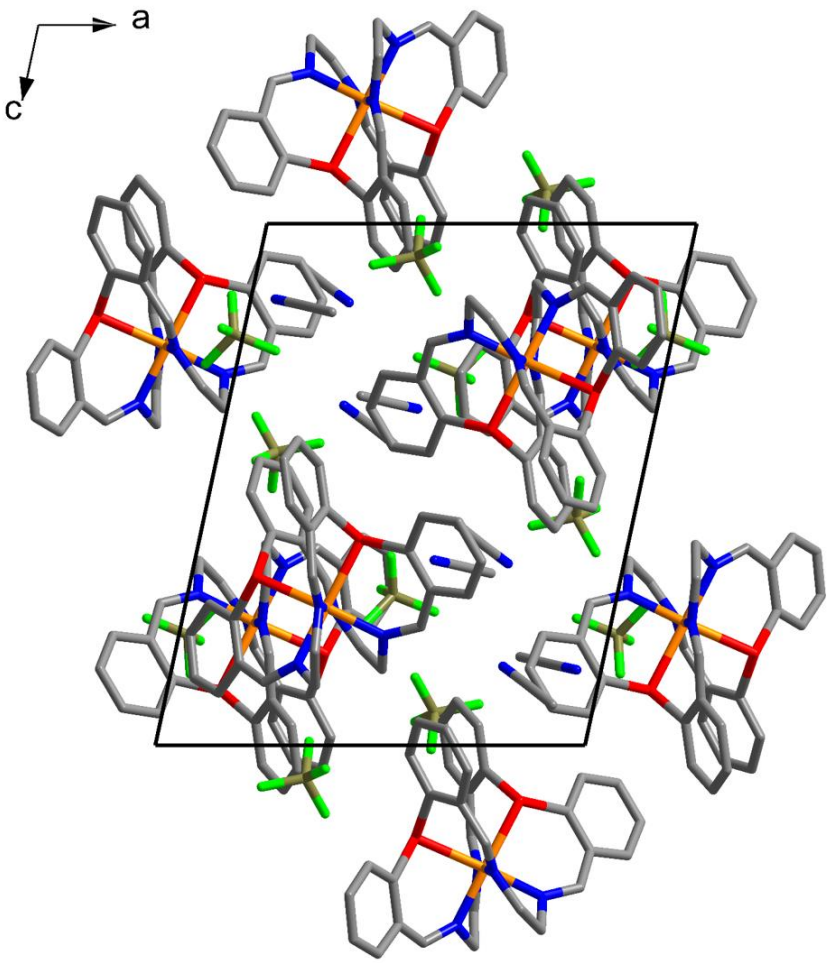

Figure S2. Packing diagram of **7**, $[C_{32}H_{28}FeN_4Se_2][BF_4]_2 \cdot 2(CH_3CN)$, along the *b*-axis, showing the coordinated macrocycle, tetrafluoroborate anions, and crystallized acetonitrile solvent molecules. Color scheme: C = gray, N = blue, Fe = orange, Se = red, B = brown, F = green.

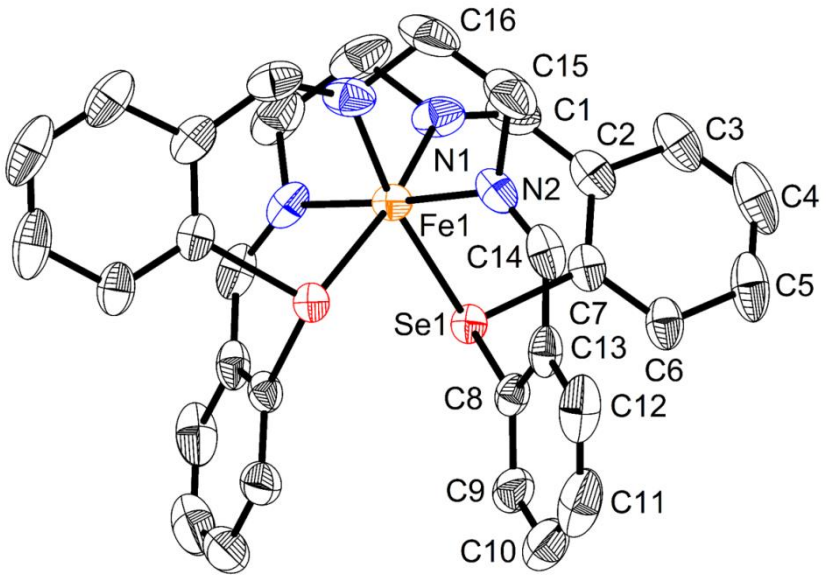

Figure S3. Structure of solvent-free $[C_{32}H_{28}FeN_4Se_2][BF_4]_2$ shown as 50% probability ellipsoids. Hydrogen atoms and counterions omitted for clarity.

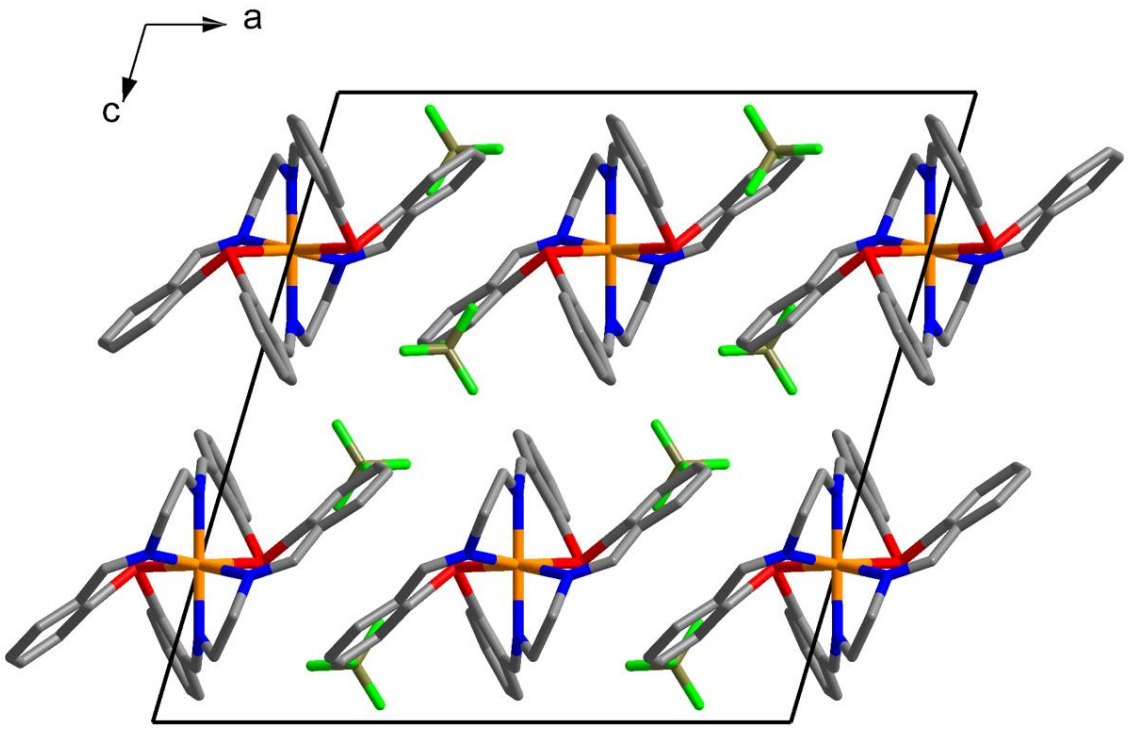

Figure S4. Packing diagram of solvent-free $[C_{32}H_{28}FeN_4Se_2][BF_4]_2$ along the *b*-axis. Color scheme: C = gray, N = blue, Fe = orange, Se = red, B = brown, F = green.

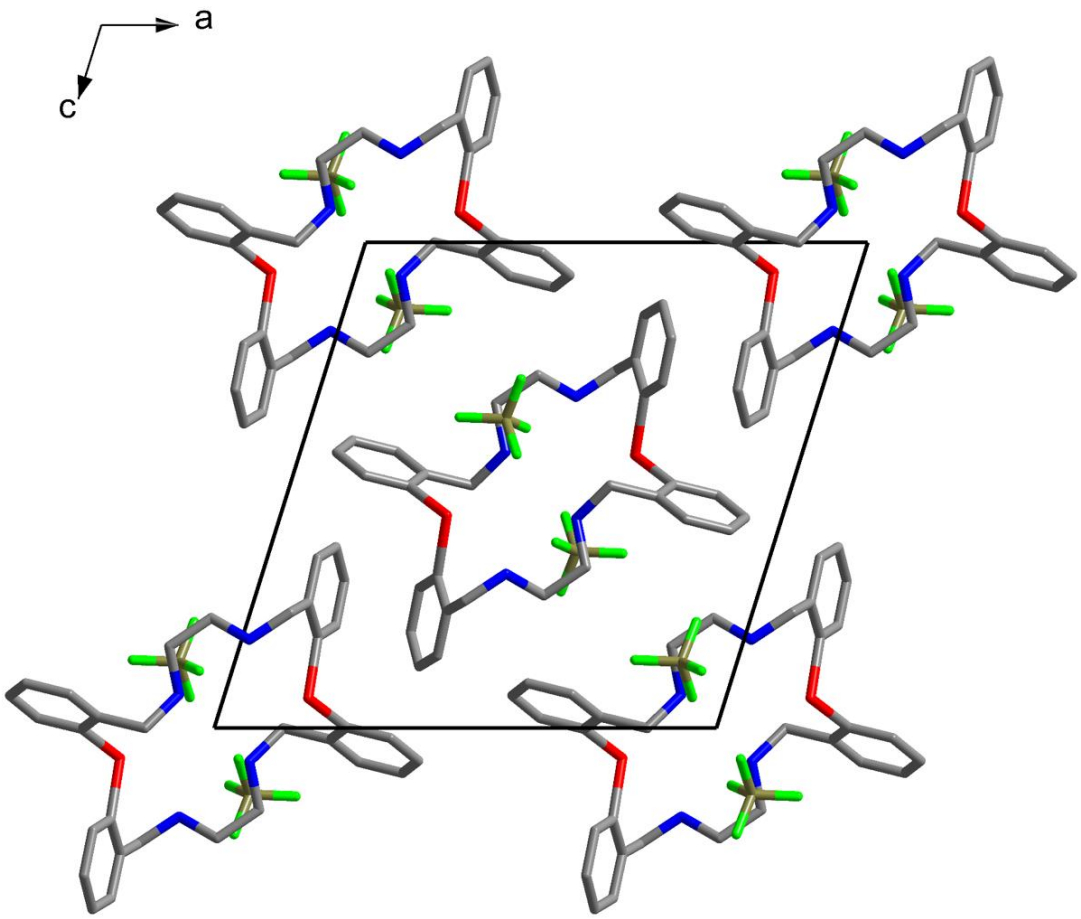

Figure S5. Packing diagram of **8**, $[C_{32}H_{38}N_4Se_2][BF_4]_2$ along the *b*-axis. Color scheme: C = gray, N = blue, Se = red, B = brown, F = green.

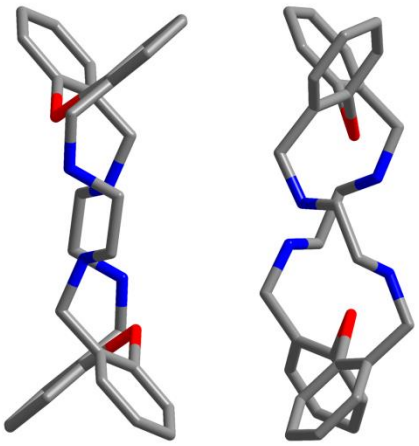

Figure S6. Comparison of the macrocycle conformation in the tetrafluoroborate-coordinated complex **8** (left) and the unbound macrocycle **6** (right). The twisting and out-of-plane bending of the Se atoms in **8** are likely necessary to properly arrange the hydrogen atoms on N2 for hydrogen bonding to the exocyclic tetrafluoroborate groups.

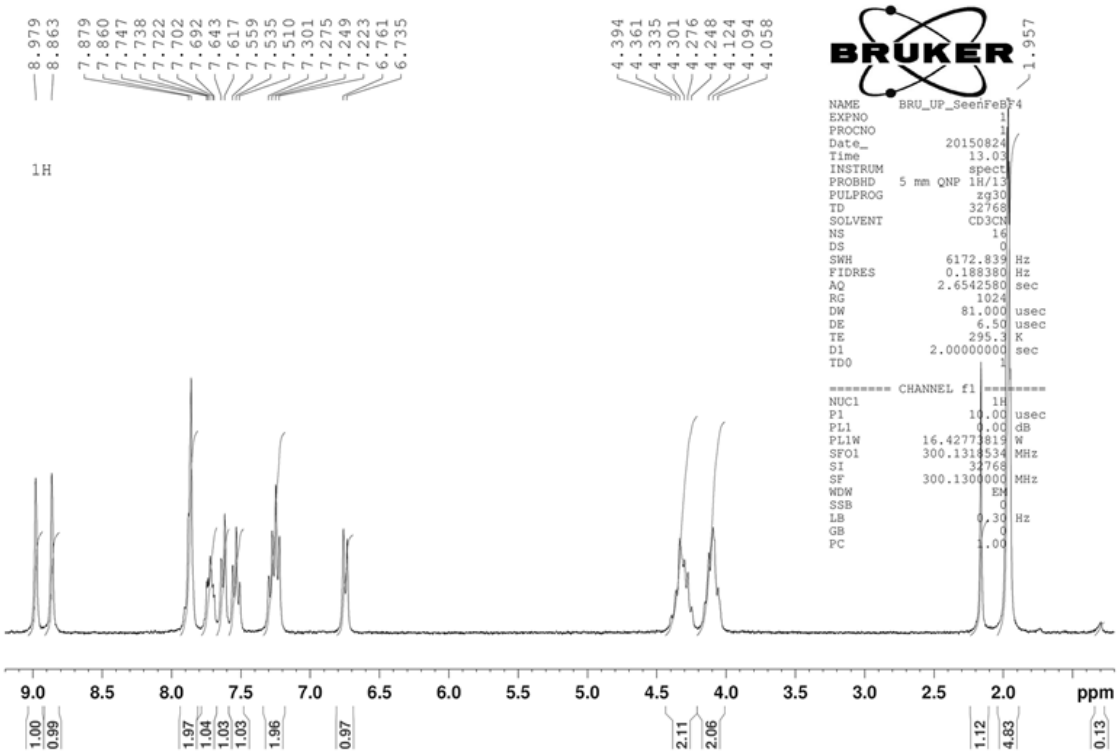

Figure S7. ^{1}H NMR spectrum of complex **7** in CD_3CN.

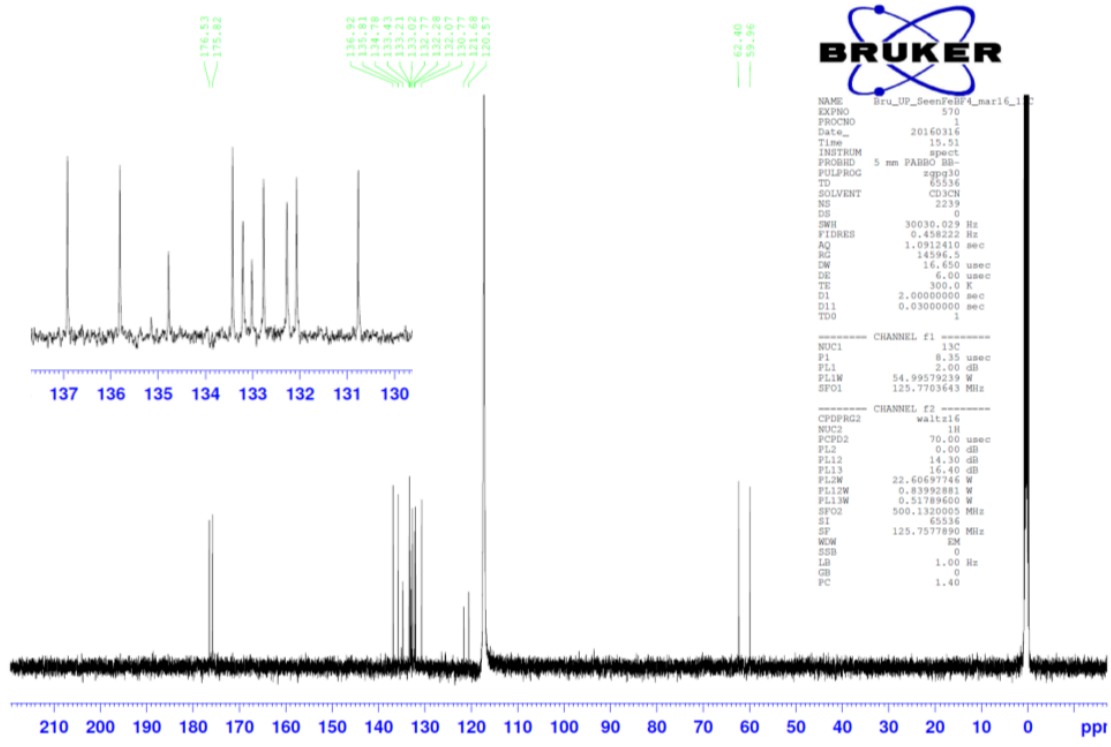

Figure S8. $^{13}C\{^{1}H\}$ NMR spectrum of complex **7** in CD_3CN with inset of aromatic region.

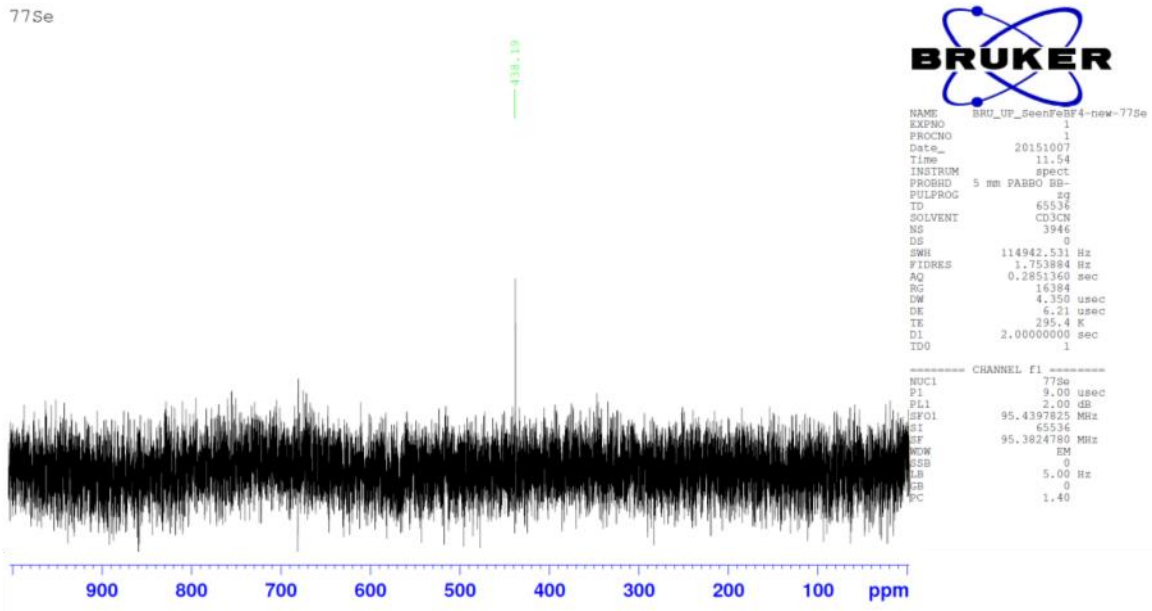

Figure S9. ^{77}Se NMR spectrum of complex **7** in CD_3CN.

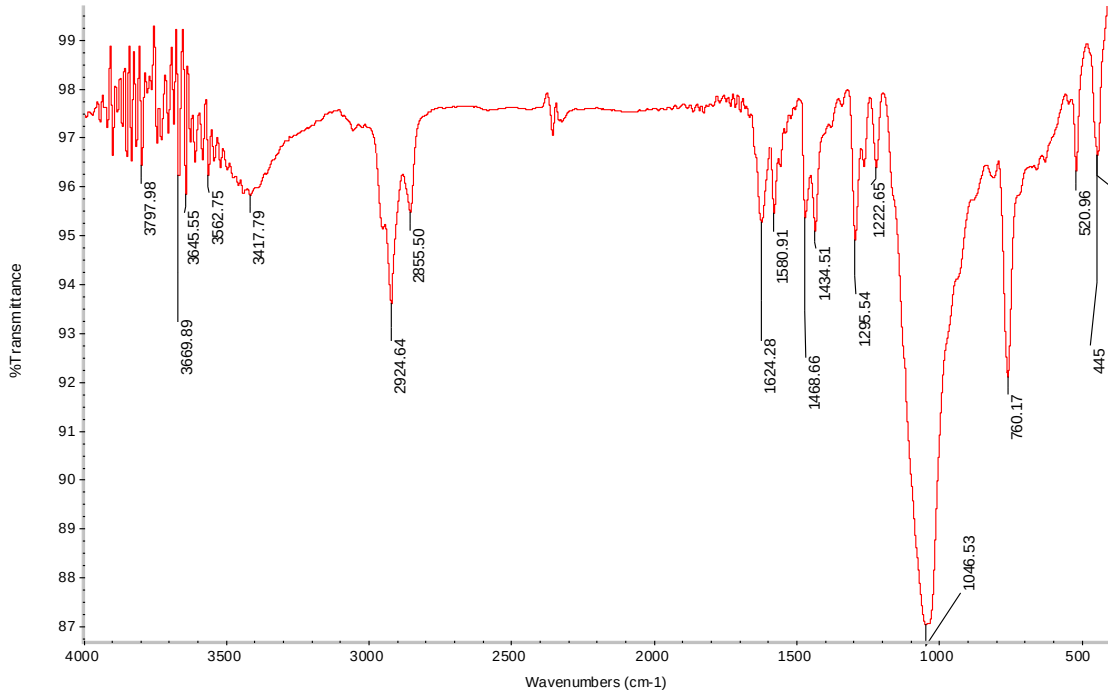

Figure S10. IR spectrum of complex **7** from a KBr pellet.

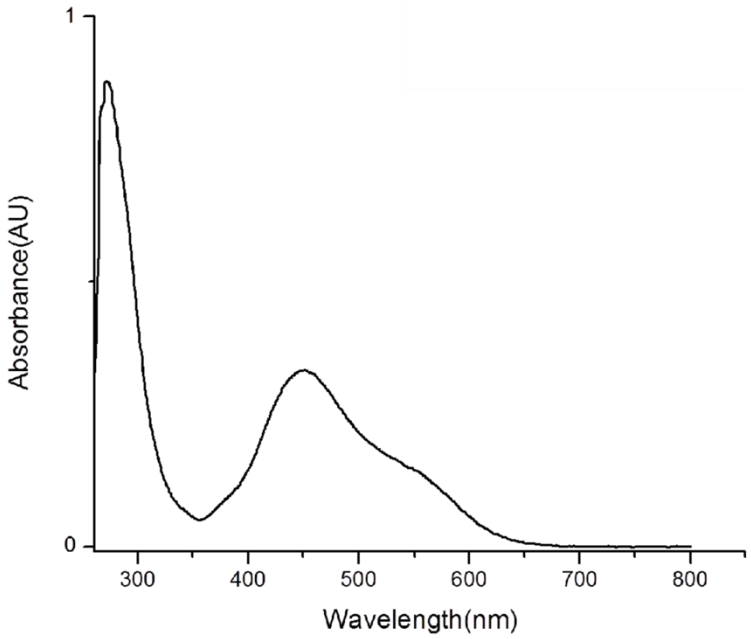

Figure S11. UV-vis spectrum of complex **7** (0.07 mM in CH_3CN).

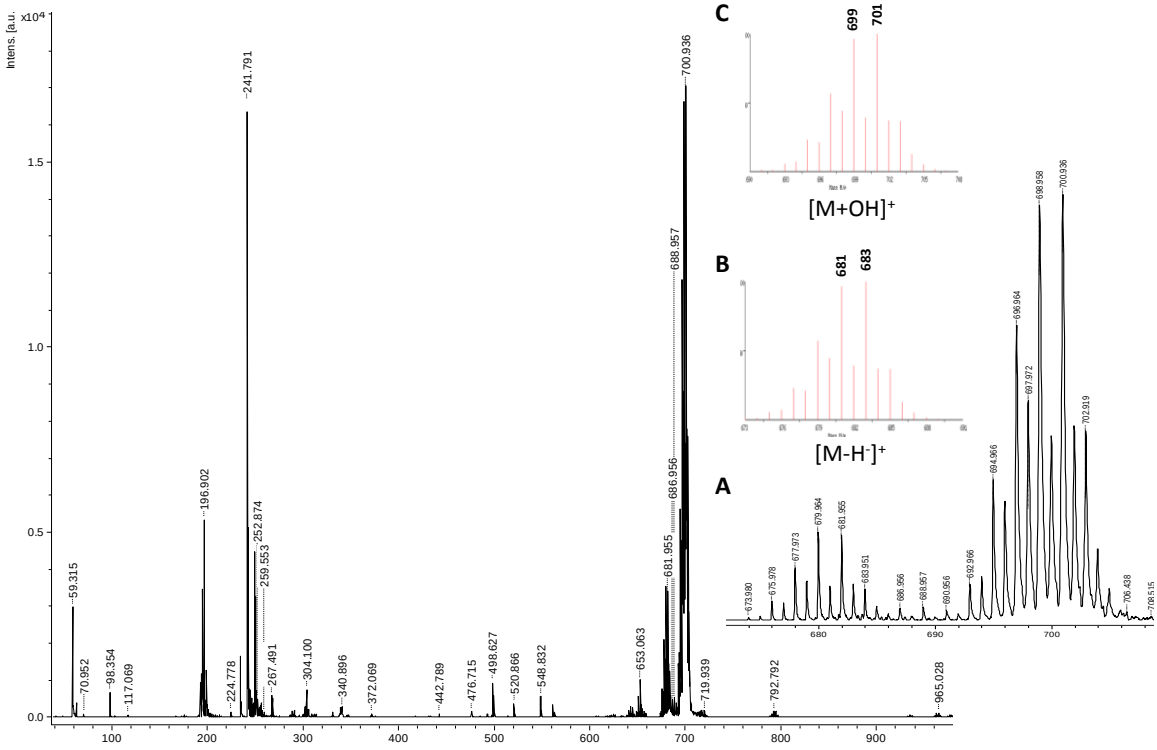

Figure S12. MALDI mass spectrum of complex **7** with A) expanded portion; B) and C) theoretical peak envelopes.

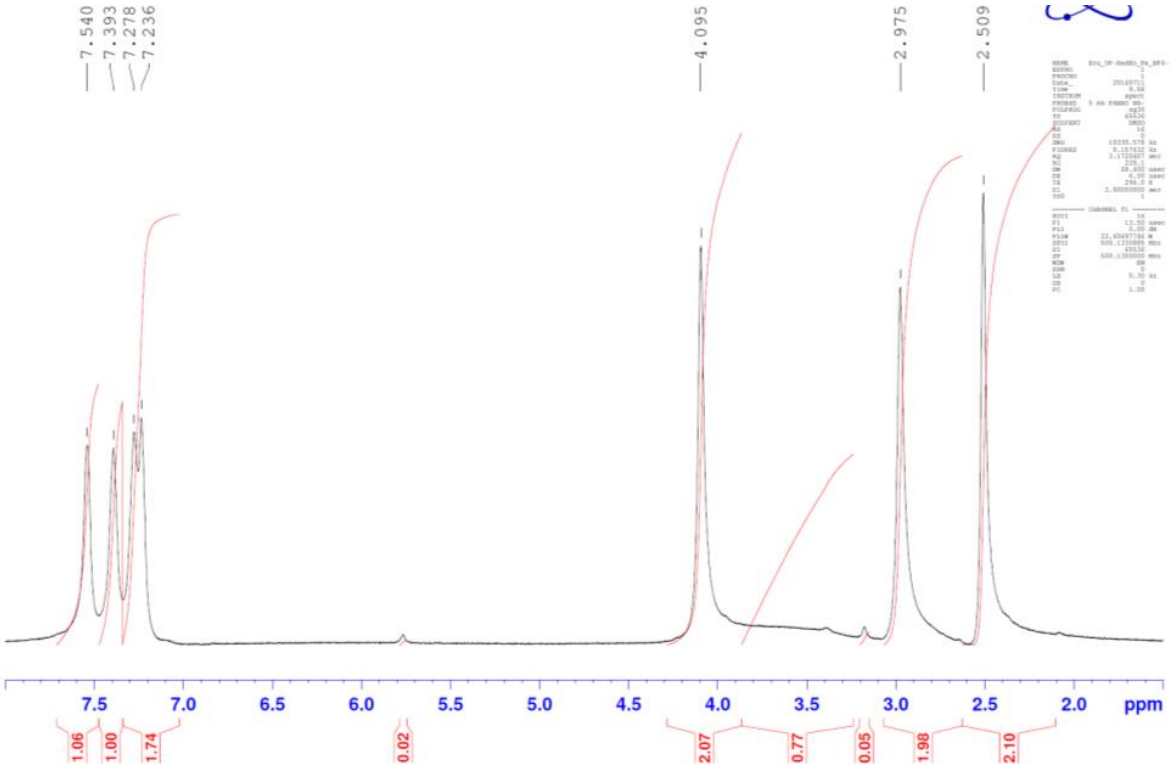

Figure S13. ^{1}H NMR spectrum of complex **8** in d_6-DMSO. No additional resonances observed from δ -0.5 to 11.

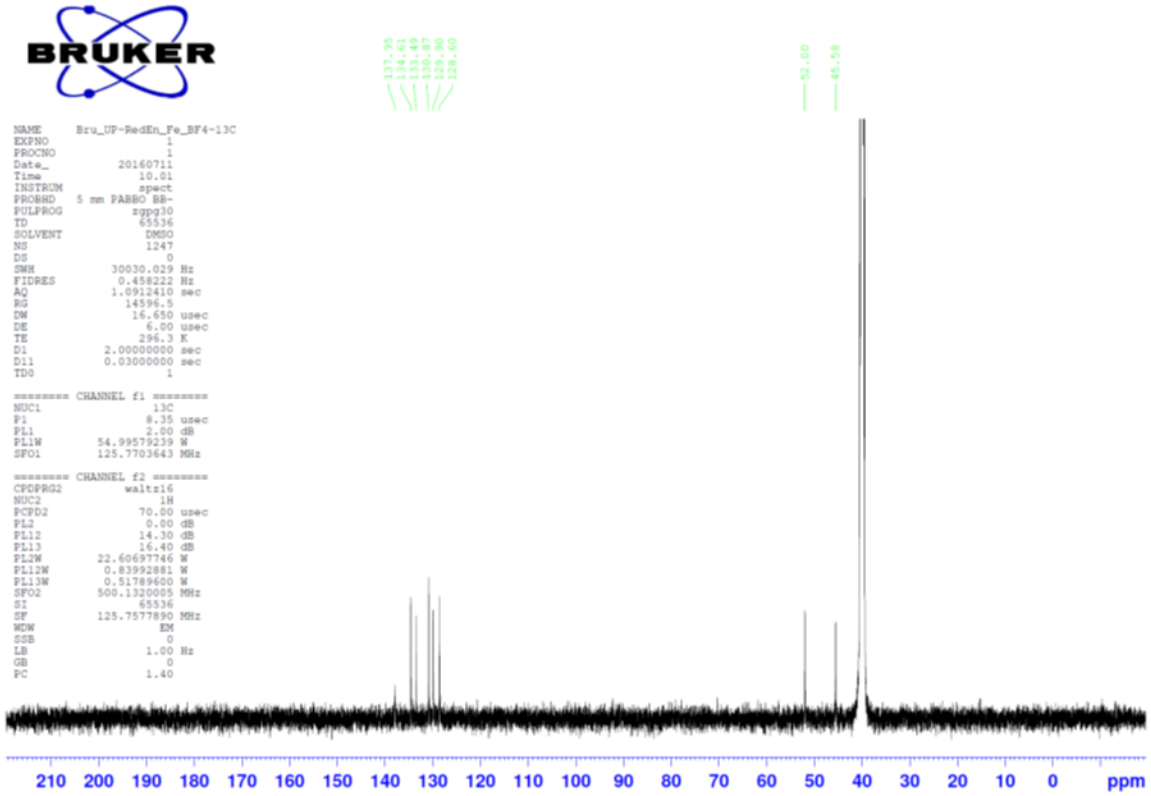

Figure S14. ^{13}C{^{1}H} NMR spectrum of complex **8** in CD_3CN.

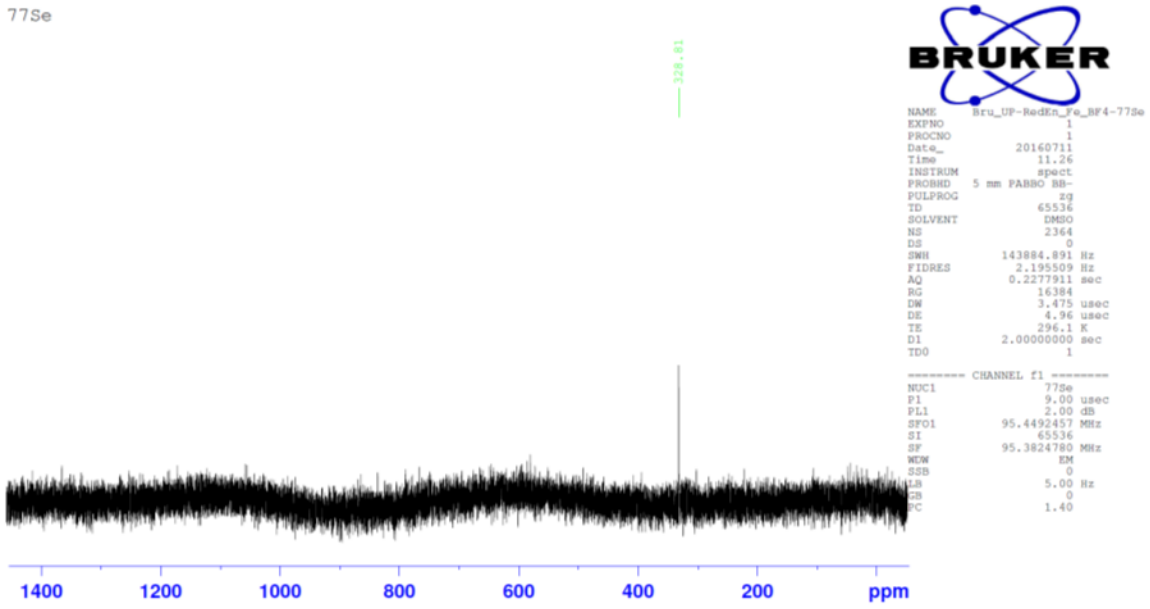

Figure S15. ^{77}Se NMR spectrum of complex **8** in d_6-DMSO.

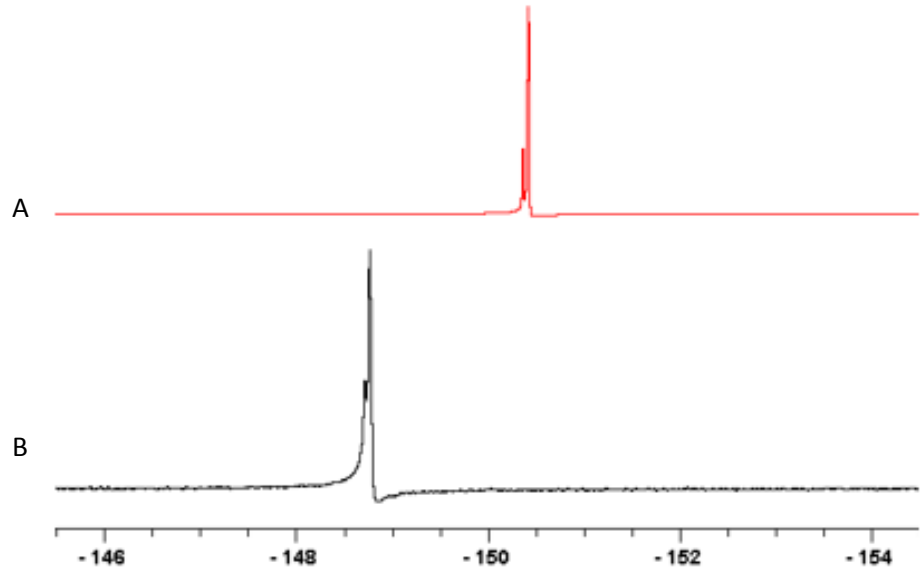

Figure S16. ^{19}F NMR spectra of A) selenomacrocyclic **6** B) complex **8** in d_6-DMSO.

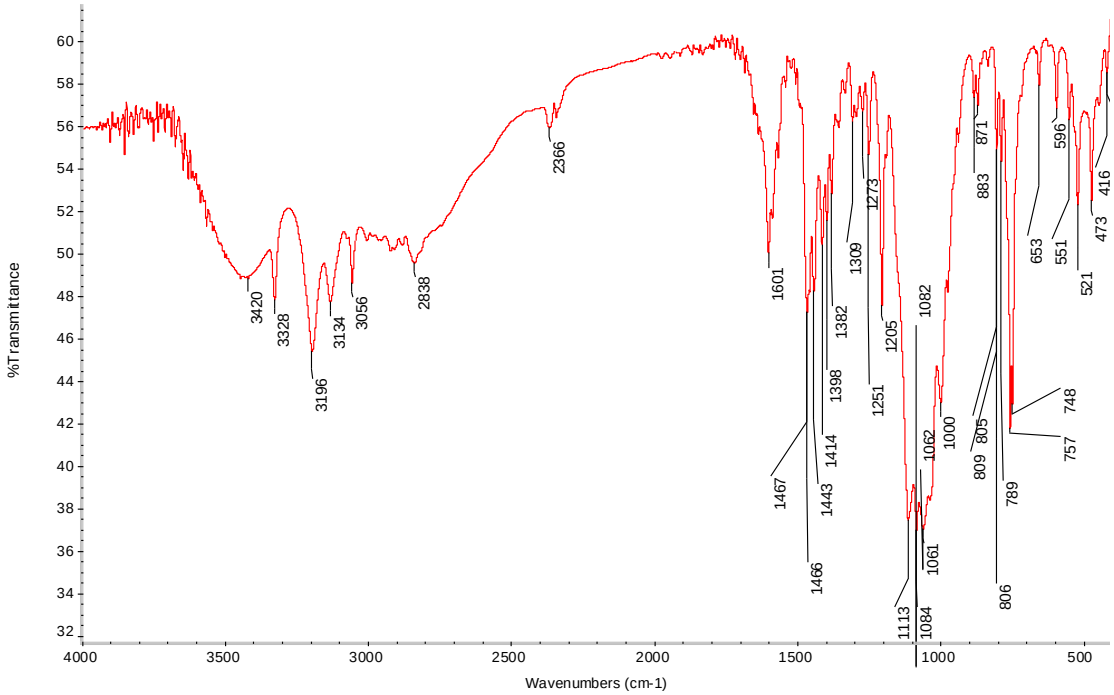

Figure S17. IR spectrum of complex **8** from a KBr pellet.

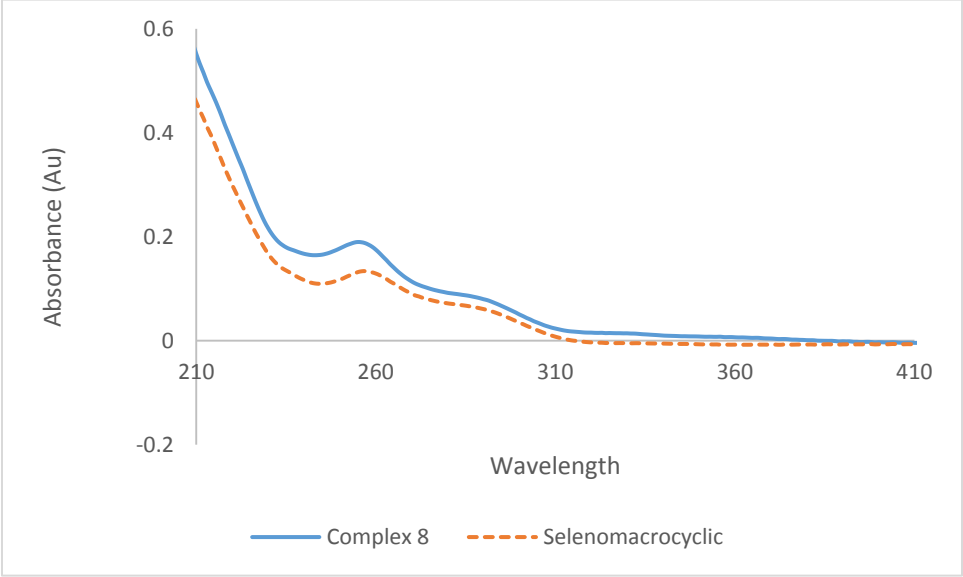

Figure S18. UV-vis spectra of selenazamacrocycle **6** and BF_4^--bound complex **8** (0.07 mM in CH_3CN).

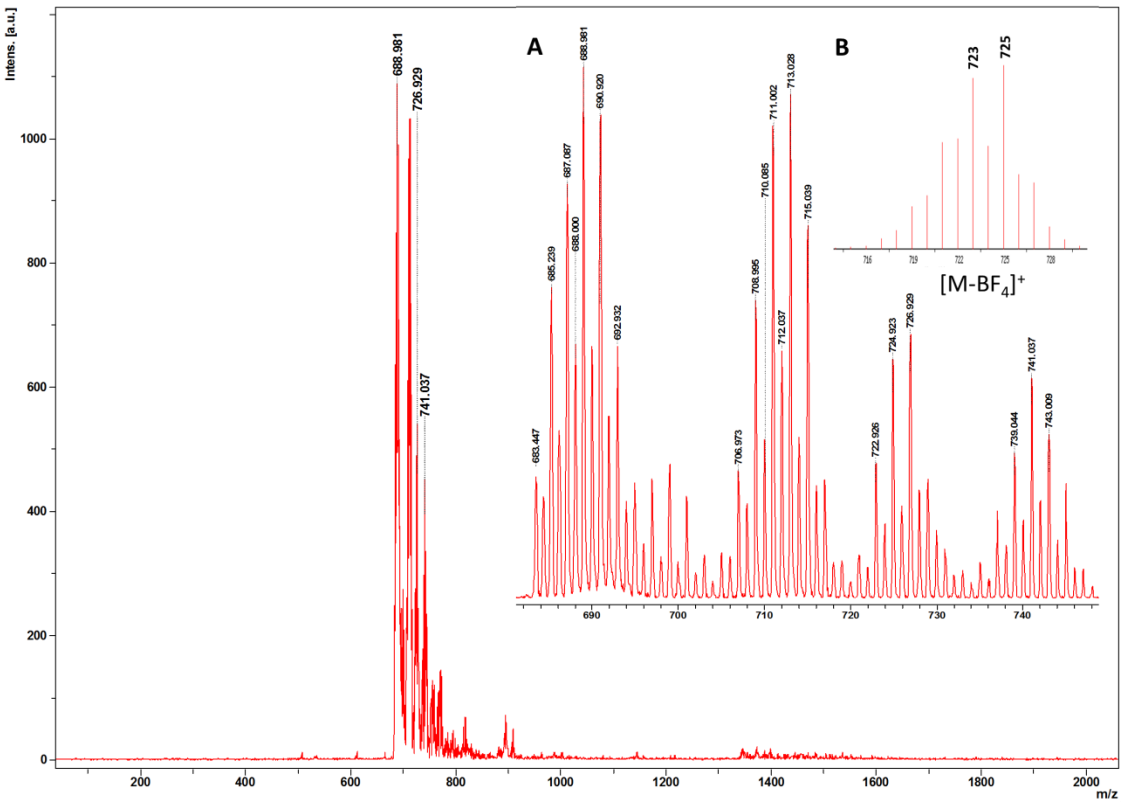

Figure S19. MALDI mass spectrum of complex **8** with A) expanded region and B) theoretical peak envelope.

References

1. A. Panda, S. C. Menon, H. B. Singh, C. P. Morley, R. Bachman, T. M. Cocker, R. J. Butcher, *Eur. J. Inorg. Chem.*, 2005, 1114-1126.
2. S. Panda, S. S. Zade, H. B. Singh, R. J. Butcher, *Eur. J. Inorg. Chem.*, 2006, 172-184.
3. J. D. Odom, W. H. Dawson, P. D. Ellis, *J. Am. Chem. Soc.*, 1979, **101**, 5815-5822.
4. M. J. Frisch, G. W. Trucks, H. B. Schlegel, G. E. Scuseria, M. A. Robb, J. R. Cheeseman, G. Scalmani, V. Barone, B. Mennucci, G. A. Petersson, H. Nakatsuji, M. Caricato, X. Li, H. P. Hratchian, A. F. Izmaylov, J. Bloino, G. Zheng, J. L. Sonnenberg, M. Hada, M. Ehara, K. Toyota, R. Fukuda, J. Hasegawa, M. Ishida, T. Nakajima, Y. Honda, O. Kitao, H. Nakai, T. Vreven, J. A. M. Jr., J. E. Peralta, F. Ogliaro, M. Bearpark, J. J. Heyd, E. Brothers, K. N.

Kudin, V. N. Staroverov, T. Keith, R. Kobayashi, J. Normand, K. Raghavachari, A. Rendell, J. C. Burant, S. S. Iyengar, J. Tomasi, M. Cossi, N. Rega, J. M. Millam, M. Klene, J. E. Knox, J. B. Cross, V. Bakken, C. Adamo, J. Jaramillo, R. Gomperts, R. E. Stratmann, O. Yazyev, A. J. Austin, R. Cammi, C. Pomelli, J. W. Ochterski, R. L. Martin, K. Morokuma, V. G. Zakrzewski, G. A. Voth, P. Salvador, J. J. Dannenberg, S. Dapprich, A. D. Daniels, O. Farkas, J. B. Foresman, J. V. Ortiz, J. Cioslowski, D. J. Fox. Gaussian 09 (Revision B.01), Gaussian, Inc.: Wallingford, CT, 2010.

5. Apex 3, Bruker AXS, Inc., Madison, WI, 2015.
6. G. Sheldrick, *Acta Crystallogr.*, 2008, **A64**, 112-122.